Present-Day Stress Orientation in Thailand's Basins

Mark R. P. Tingay[1,*], Chris K. Morley[2], Richard R. Hillis[3], Jeremy Meyer[4]

[1] Department of Applied Geology, Curtin University of Technology, WA, Australia.

* Corresponding author. Tel.: +61 8 9266 7097; fax: +61 8 9266 3153, Email address: m.tingay@curtin.edu.au

[2] PTT Exploration and Production, Bangkok, Thailand.

[3] Australian School of Petroleum, University of Adelaide, Adelaide, Australia.

[4] JRS Petroleum Research, Adelaide, Australia.

Abstract

The Cenozoic tectonic evolution of Thailand is widely considered to have been primarily controlled by forces generated at the eastern Himalayan syntaxis. This hypothesis is supported by earthquakes in northern Indochina and southern China, which reveal a fan shaped present-day maximum horizontal stress (S_{Hmax}) pattern centered on the eastern Himalayan syntaxis. However, the distance to which forces generated by the Himalayan syntaxis influence the stress pattern in Indochina is not known. We analyzed caliper and image logs from 106 petroleum wells for borehole breakouts and drilling-induced fractures. A total of 558 breakouts and 45 drilling-induced fractures were interpreted in six basins, indicating that a north-south regional present-day S_{Hmax} exists in central and southern Thailand and the Gulf of Thailand. The N-S S_{Hmax} orientation suggests that forces generated at the Himalayan syntaxis are a major control on the stress pattern throughout Thailand, extending approximately 1000 km beyond the outer limit of syntaxis-associated seismicity. Despite the influence of the Himalayan syntaxis on the present-day stress field, the sedimentary basins of central, southern and offshore Thailand are characterized by structural styles that are somewhat inconsistent with those predicted to result from India-Eurasia collision. Furthermore, localized variations in S_{Hmax} orientation, and the

predominance of structures associated with purely extensional rifting, indicate that other processes also influence the stress field in Thailand. We suggest that stresses generated by the Sumatran-Andaman subduction zone may also have resulted in significant deformation in offshore Thailand and that the stress pattern may also be perturbed at very local (several km) scales by mechanically weak faults.

Key words: Present-day Stress; Thailand; Borehole Breakout; Neotectonics.

Introduction

Thailand lies in the heart of one of the most tectonically active regions on Earth and displays an extensive history of Cenozoic deformation (Morley, 2002; Hall & Morley, 2004). Consequently the present-day stress field provides insight into a region of continental crust that is actively deforming (Morley, 2001; Tingay et al., *in press*). Understanding present-day stress orientations is important for several reasons including: testing tectonic and fault evolution models for the region, hazard prediction associated with fault reactivation, and for the petroleum industry with regard to borehole stability and predicting the orientation of open fracture systems (Hall and Morley, 2004; Morley et al., 2004; Vigny et al., 2005; Tingay et al., 2009).

The Cenozoic tectonic evolution of Indochina is often considered to be controlled by stresses and strains arising from the ongoing collision of India with Eurasia (Molnar & Tapponnier, 1975; Morley, 2002; England & Molnar, 2005). The nature of Himalayan extrusion into SE Asia remains a topic of debate, with some authors proposing rigid block escape tectonics (Molnar & Tapponnier, 1975; Tapponnier et al., 1982; Leloup et al. 2001; Replumaz and Tapponier 2003) whereas other authors suggest that deformations can be better matched by viscous or visco-elastic flow (England & Molnar, 2005; Shen et al., 2005). Regardless of the nature of Himalayan

extrusion, all models predict a fan-like present-day maximum horizontal stress (S_{Hmax}) pattern in Indochina centered on the eastern Himalayan syntaxis, with present-day S_{Hmax} oriented NNW-SSE to NNE-SSW throughout much of Indochina (Huchon et al., 1994; Kong & Bird, 1997; Morley, 2007). The modeled NNW-SSE to NNE-SSW S_{Hmax} orientation in Indochina is supported by stress orientations estimated from earthquake focal mechanisms solutions in northern Thailand and the Yunnan Region of China (Fig. 1; Holt et al., 1991; Huchon et al., 1994; Morley et al., 2001; Morley, 2007). However, there is a relative absence of seismicity south of approximately 17ºN latitude in Indochina and thus it is not known whether the fan-shaped stress pattern observed in regions adjacent to the Himalayan syntaxis extends into southern Thailand and offshore Indochina.

Models of extrusion tectonics predict different distances at which forces generated at the Himalayan syntaxis should influence the stress field in SE Asia (Molnar & Tapponnier, 1975; Morley, 2002; Hall & Morley, 2004). For example, the rigid block escape tectonics model predicts that the stress pattern, and associated deformations, throughout much of the Sunda plate would be controlled by Himalayan extrusion (Molnar & Tapponnier, 1975; Huchon et al., 1994). However, the Cenozoic tectonic evolution of Indochina has also been strongly influenced by processes other than Himalayan extrusion, most notably stresses arising from the Java-Sumatra-Andaman subduction zone to the south and west of Thailand, gravitational collapse of thickened continental crust in Indochina and the coupling between the Burma block in Myanmar with India (Morley, 2001; Hall & Morley, 2004; Morley et al., *in press*; Searle & Morley, *in press*). Hence, the primary aim of this study is to determine the present-day S_{Hmax} orientation in central and southern Thailand and the Gulf of Thailand (south of 17ºN latitude) in order to better establish the forces controlling the present-day stress field in Indochina and examine the distance at which forces generated by the Himalayan syntaxis influence the stress pattern in SE Asia.

Thailand displays some exceptional examples of extensional fault geometries that can be seen from satellite images, open cast coal mines and from 2D and 3D reflection seismic data (e.g. Rigo de Rhigi et al., 2002; Uttamo et al., 2003; Morley et al., 2004). These fault patterns commonly display multiple orientations, and complex fault propagation and linkage patterns that indicate inheritance of older fabrics, and complex evolution of the stress field with time (e.g. Morley and Wonganan, 2000; Kornsawan and Morley 2002; Morley et al., 2004; Morley et al., 2007). Investigation of the modern stress field can help determine whether fault orientations oblique to the main rift trend can be explained by simple reactivation of deeper structures, or whether other factors, such as localized stress rotations need to be considered. Hence, a secondary aim of this study is to examine the stress field at small-scales within sedimentary basins in order to investigate whether complex fault patterns in Thailand may be the result of local stress perturbations or the reactivation of deeper structures.

Geological Summary

Central and southern Thailand and the Gulf of Thailand are tectonically significant regions of Southeast Asia because they lie along the north-south transition from the orogenic region of the Himalayan syntaxis to the subduction-dominated Java-Sumatra margin further south. The tectonic development of Indochina is often considered to be dominated by widespread, large-scale strike-slip faulting associated with Himalayan extrusion tectonics (Tapponier & Molnar, 1975; Tapponnier et al., 1986). More recent work has, however, established that the Cenozoic tectonic evolution of Thailand is considerably more complex (Hall and Morley, 2004; Morley et al., *in press*; Searle & Morley, *in press*). The geography of Thailand very strongly expresses Cenozoic deformation that can be divided into seven main provinces, three in the south and four in the north (Morley et al., *in press*). The three southern provinces comprise Peninsular Thailand,

101 the Gulf of Thailand and the Andaman Sea, whilst the northern provinces consist of the Western
102 Highlands, the central region, northern central region and the Khorat Plateau (Fig. 1). The
103 provinces are described below from south to north.
104
105 The Gulf of Thailand is dominated by Cenozoic rift systems, and has been an area of subsidence,
106 and extensive sedimentation since the Eocene (e.g. Lockhart et al., 1997; Jardine, 1997, Morley
107 and Westaway, 2006). Some basins are large, extremely deep and subsided rapidly, such as the
108 super-deep Pattani and Malay Basins, which in places contain over 7 km of Neogene section
109 (Morley & Westaway, 2006). The present day shape of the gulf is due to a sea-level highstand
110 covering an extensive, broadly subsiding intra-continental post-rift basin (maximum water depth
111 of 80 m), which extends onshore as the Central Basin.
112
113 The Andaman Sea is a region affected by Late Oligocene-Early Miocene transtension, followed
114 by Early Pliocene sea floor spreading in a pull-apart setting (Khan and Chakraborty, 2005).
115 Major N-S dextral strike-slip was initiated when western Myanmar became coupled to India and
116 was dragged northwards (along the Sagaing Fault) with respect to both Sumatra to the south, and
117 Peninsular Thailand to the east (see review in Curray, 2005). In contrast with the subdued Gulf of
118 Thailand bathymetry, the Andaman Sea is a large back-arc region with bathymetry related to the
119 Sumatra-Andaman plate boundary, strike-slip fault margins, and rifted passive-margins flanking
120 a deep marine back-arc spreading centre (maximum water depth 3,777 m).
121
122 Peninsular Thailand is a hilly strip of narrow highlands uplifted during the Cenozoic (particularly
123 the Late Oligocene to early Miocene; Upton, 1999). It is only a narrow strip of land due to late
124 Cenozoic tectonic processes driving subsidence in the Andaman Sea area to the west, and the
125 Gulf of Thailand to the east. The peninsula also contains a few small rift basins (e.g. Surat Thani

126 Basin) and is cut by two major NE-SW trending Cenozoic dextral strike-slip faults (Khlong
127 Marui and Ranong faults; Fig. 1).
128
129 The central region, in which Bangkok is located, forms a broad flat plain (Central Plains) that
130 narrows northwards. The plains are 450 km long, up to 125 km wide and range in elevation from
131 sea level to 50 m. The central region plains are a remarkable expression of an extensive, young,
132 post-rift (thermal subsidence) basin called the Chao Phraya Basin. This basin began to
133 unconformably cover the Late Oligocene-Miocene rift basins (Phitsanulok, Kampaeng Saeng and
134 Suphan Buri Basins) and intervening pre-Cenozoic rocks during the Late Miocene or early
135 Pliocene (Morley et al., 2007).
136
137 East of the Central Plains region is the Khorat Plateau, which is a low-topography area lying at
138 ~500 m elevation, underlain by ~3000-4000 m thickness of predominately sub-horizontal
139 Mesozoic continental clastics of the Khorat Group (Kozar et al., 1992). The Khorat Group is
140 affected by variably trending Cenozoic folds that in some areas give rise to hilly topography,
141 most notably around the western margin of the Khorat Plateau and the Phu-Phan uplift (Fig. 1).
142 Apatite fission track dating of the Khorat Group in the more strongly folded areas indicates
143 exhumation linked with rising folds occurred between about 50 Ma and 30 Ma (Upton, 1999).
144
145 West of the Central Plains region is the Shan Plateau, an uplifted region straddling eastern
146 Myanmar and Western Thailand composed predominantly of Palaeozoic sedimentary and
147 metasedimentary rocks extensively intruded by Mesozoic and early Cenozoic granites. The
148 western highlands in Thailand mark the eastern limit of the Plateau. Typical maximum elevations
149 in the Plateau area are ~1500 m. The western extent of the Plateau is sharply defined by the Shan
150 Scarp and the adjacent N-S striking Sagaing Fault (Fig. 1). The Sagaing Fault is one of the

largest and most active strike-slip faults in the world, with dextral motion in the order of ~2.0 cm/yr (Vigny et al., 2003). That motion accommodates about two thirds of the northwards motion of India relative to Indochina. On satellite images the plateau is spectacularly cross-cut by a network of predominantly N-S and NW-SE trending major Cenozoic strike-slip faults that are clearly visible as linear topographic features (e.g. Le Dain et al,. 1984, Lacassin et al., 1997, Lacassin et al., 1998, Morley, 2004). The NW-SE striking Mae Ping and Three Pagodas Fault zones are the best developed of these strike-slip fault zones in Thailand. During the Paleogene they underwent major (>100 km), sinistral motion, while minor (up to a few tens of kilometers) dextral displacement occurred during the Late Oligocene and Neogene (Lacassin et al., 1997; Morley, 2004).

The Cenozoic rift trend passes from the central plains region into northern Thailand, however extensional activity continued into more recent times in the north where some faults remain active today (Bott et al., 1997, Fenton et al., 1997, Fenton et al., 2003). The northern rifts are characterized by over forty intermontane rift basins forming isolated plains (Fig. 1) that lie at elevations between 200 m and 500 m. These basins retain their syn-rift topography, with the intermontane plains flanked by high hills with elevations up to 1500 m, composed predominantly of Palaeozoic-Early Mesozoic rocks (Morley et al., *in press*).

The Cenozoic rift basins of central, western, northern and offshore Thailand are highly variable in size, with many being only 10s-100s km^2 in size and 10s to 100s of meters deep. The N-S orientation of these basins has been suggested to indicate that they are purely the result of Himalayan extrusion, with the basins forming as pull aparts due to displacement along major NW-SE trending faults (Tapponnier et al., 1986; Polachan et al., 1991). Some basins in western and northern Thailand do appear to have a strike-slip or oblique extension origin, but basins

176 further to the south and east grade into extensional basins where a purely strike-slip origin can be
177 disproved (Morley, 2001; Morley, 2007). Furthermore, Cenozoic strike-slip deformation has
178 arisen from both deformation at the eastern Himalayan syntaxis (Huchon et al., 1994; Kong &
179 Bird, 1997) and from coupling of the Indian Plate with the Burma block that introduced a N-S
180 trending broad dextral shear couple on western Thailand and eastern Burma from the Oligocene
181 onwards (e.g. Curray, 2005). Other forces that potentially acted on Thailand during the Cenozoic
182 are from the Sumatran-Andaman subduction zone and buoyancy forces associated with
183 thickening of the continental crust during the Late Cretaceous and Paleogene (Morley, 2001; Hall
184 and Morley, 2004; Morley et al., *in press*; Tingay et al., *in press*).
185
186 That the Cenozoic tectonic evolution of Thailand has been influenced by a complex interplay of
187 different forces, and is not purely a consequence of India-Eurasia collision, is suggested by both
188 the spatial variations in deformation style described above and the evolution of structures over
189 time. Oligocene-Miocene rift basins are developed over folds, thrusts and strike-slip faults
190 formed during the Paleogene (Morley, 2007; Morley et al., 2007; Morley et al., *in press*). Pull-
191 apart basins in western Thailand that developed during the Late Oligocene-Early Miocene are
192 associated with a change from sinistral to dextral strike-slip motion along major NW-SE to N-S
193 trending faults (Morley, 2004). The pull-apart basins appear to have ceased activity during the
194 Middle Miocene, while extensional basins to the east continued to be active (Lacassin et al.,
195 1997; Morley, 2007). Several Miocene-Pliocene stress changes can be inferred in the rift basins,
196 both as variations in dominant fault orientation over time and by alternating phases of inversion
197 and extension (Lacassin et al., 1997; Morley, 2007; Morley et al., 2007; Morley et al., *in press*).
198 Most significantly for the modern stress regime is that a final phase of widespread basin
199 inversion occurred around the Miocene-Pliocene boundary, after which time extension stopped or
200 was greatly reduced in most onshore rift basins (Morley et al., 2001).

Determination of Present-Day Maximum Horizontal Stress Orientation

The present-day stress tensor in sedimentary basins is conventionally simplified to consist of four components: the vertical stress magnitude, S_{Hmax} magnitude, minimum horizontal stress magnitude and S_{Hmax} orientation (Bell, 1996). The vertical, maximum and minimum horizontal stresses are typically assumed to be principal stresses, particularly in sedimentary basins that generally have little topographic variation (Bell, 1996). Herein, we focus primarily on determining the S_{Hmax} orientation, which is assumed to represent a principal stress. Present-day S_{Hmax} orientations in Thailand's basins were determined from borehole breakouts and drilling-induced fractures (DIFs) interpreted from four-arm caliper and resistivity image log data. When a borehole is drilled, the material removed from the subsurface is no longer supporting the surrounding rock. As a result, the stresses become concentrated in the surrounding rock (i.e. the wellbore wall; Kirsch, 1898). Borehole breakouts are stress-induced elongations of the wellbore and occur when the wellbore stress concentration exceeds that required to cause compressive failure of intact rock (Bell & Gough, 1979). The elongation of the cross-sectional shape of the wellbore is the result of compressive shear failure on intersecting conjugate planes, which causes pieces of the borehole wall to spall off (Bell & Gough, 1979). The maximum circumferential stress around a vertical borehole occurs perpendicular to the maximum horizontal stress (Kirsch, 1898). Hence, borehole breakouts are elongated perpendicular to the maximum horizontal stress direction (Bell & Gough, 1979).

Drilling-induced fractures are caused by tensile failure of the borehole wall and form when the wellbore stress concentration is less than the tensile strength of the rock (Aadnøy, 1990). The minimum circumferential stress around a vertical borehole occurs in the direction of the

maximum horizontal stress (Kirsch, 1898). Hence, DIFs are oriented in the S_{Hmax} direction (Aadnøy & Bell, 1998).

Breakouts are interpreted herein from the Schlumberger High-Resolution Dipmeter Tool (HDT) and Oil-Based Dipmeter Tool (OBDT) logs and resistivity image logs. The HDT and OBDT are four-arm caliper tools with two pairs of caliper arms at 90° to each other. Each arm has a pad on the end containing one or two resistivity 'buttons'. The resistivity data from four-arm caliper tools are processed to obtain information about the formation (primarily dip and strike of bedding) and to calculate hole volume (Schlumberger, 1986). However, borehole breakouts can be interpreted from unprocessed HDT log data. The logs used to interpret breakouts from the HDT are the:

- borehole deviation (DEVI) and azimuth (HAZI);
- azimuth of pad one (P1AZ);
- bearing of pad one relative to the high side of the hole (RB), and;
- diameter of the borehole in two orthogonal directions ('caliper one' (C1) given by arms one and three and 'caliper two' (C2) from arms two and four).

The tool tends to rotate as it is pulled up the borehole due to the lay of the cable (cable torque). However, the tool stops rotating where the cross-sectional shape of the borehole is elongated when one caliper pair becomes 'stuck' in the elongation direction (Fig. 2; Plumb & Hickman, 1985). The combined use of the six logs listed above allows the interpreter to identify zones of borehole breakout and the orientation of the elongation (Fig. 2). Many non-circular wellbore cross-sectional shapes are not stress-induced, such as washout and key-seating (Plumb & Hickman, 1985). Borehole breakout is distinguished from other borehole elongations on HDT logs using a strict set of criteria presented in Table 1 (Plumb & Hickman, 1985).

Resistivity image logs evolved from the four-arm dipmeter logs. There are a number of resistivity buttons on each pad of the resistivity image tool, for example 16 buttons per pad on Schlumberger's Formation Micro Scanner (FMS). The multiple resistivity buttons provide an image of the borehole wall based on resistivity contrasts (Fig. 2; Ekstrom et al., 1987). Resistivity image tools also measure the hole size and logs obtained by the HDT. Several types of resistivity image tools are available. However, only Schlumberger's FMS and Formation Micro Imager (FMI) were used in this study. The FMI tool is an improved version of the FMS tool that has 24 resistivity buttons on each pad and a flap attached to each pad with a further 24 buttons, thereby giving greater coverage of the wellbore wall.

The resistivity image of the wellbore wall allows for a more reliable interpretation of breakouts than can be made by using dipmeter data alone (Heidbach et al., *in press*). Drilling-induced fractures can also be recognised on image logs (DIFs cannot be interpreted on four-arm caliper logs). Breakouts appear on resistivity image logs as broad, parallel, often poorly resolved conductive zones separated by 180° and exhibiting caliper enlargement in the direction of the conductive zones. DIFs appear on image logs as narrow, well defined, conductive fractures (Fig. 2; Tingay et al., 2008).

Breakouts and DIFs can rotate in inclined boreholes and do not always directly yield the horizontal stress orientation (Mastin 1988; Peska & Zoback 1995). However, the current state of stress in Thailand is believed to be a normal or strike-slip faulting stress regime (Meyer, 2003; Morley, 2004). Breakouts and DIFs do not show any significant rotation in orientation and still yield the approximate S_{Hmax} orientation in boreholes with less than 20° deviation in a normal or

strike-slip faulting stress regime (Peska & Zoback 1995). Hence, breakouts and DIFs were only used to estimate the S_{Hmax} direction in wellbore intervals with deviations of less than 20°.

The mean S_{Hmax} orientation from each well was given a quality ranking according to the World Stress Map Project criteria with A-quality being the highest (S_{Hmax} reliable to within ±15º) and E-quality the lowest (no reliable orientation determinable; Heidbach et al., *in press*). Table 2 lists the quality ranking criteria for breakouts and DIFs interpreted from image and four-arm caliper logs.

Present-Day Maximum Horizontal Stress Orientation in Thailand Basins

We analyzed four-arm caliper and resistivity image logs for borehole breakout and DIFs in 106 wells from sedimentary basins covering 1000 km N-S extent through central, southern and offshore Thailand. A total of 124.6 kilometers of four-arm caliper logs and image logs were examined in six onshore and offshore basins, including 6019 meters of image log data from nine wells (Table 3). Borehole breakouts and/or DIFs were observed in 76 wells (Fig. 3; Table 3; data for individual wells freely available from the World Stress Map Project). A total of 558 breakouts and 45 DIFs with a combined length of 12085 meters were interpreted across the six regions (Figs. 3 and 4; Table 3). Image and four-arm caliper logs were also examined in 30 wells that either did not contain breakouts/DIFs or were deviated by >20º and thus were not used herein (ranked E-quality; Table 3). The observed breakouts and DIFs indicate that S_{Hmax} is, as regional averages, oriented N-S to NNW-SSE in all six basins with standard deviations of between 23-45º (Fig. 4; Table 3). Tingay et al. (*in press*) undertook statistical analysis of the stress orientations within each basin using the Rayleigh Test to confirm the confidence level at which the null hypothesis of stress orientations being random within a province can be rejected (Coblentz & Richardson, 1992). The null hypothesis can be rejected in all six basins at a confidence level of at

least 97.5%, indicating that the average stress orientations for each basin can be reliably used as regional stress orientations (Tingay et al., *in press*). However, it is important to note that there is a significant amount of localized stress variation in several basins, the origins of which are discussed below. Furthermore, aside from some examples discussed below, borehole breakouts and DIFs observed within individual wells generally show fairly consistent orientations with depth.

Discussion

Implications of the Regional Stress Pattern for Deformation Resulting from India-Eurasia Collision

The majority of previously published present-day stress orientations for Thailand and Indochina have been derived from earthquake focal mechanism solutions that indicate a curvilinear fan-shaped stress pattern emanating from the eastern Himalayan syntaxis, with NNW-SSE to NNE-SSW S_{Hmax} orientations within northern Indochina (Figure 1; Bott et al., 1997; Morley, 2007). Hence, the N-S average S_{Hmax} orientations observed in the onshore Phitsanulok, Khorat and Suphan Buri Basins are consistent with the stress orientations observed from earthquake focal mechanisms solutions in northern Thailand (Figs. 1, 3 and 4; Morley, 2007; Tingay et al., *in press*). Present-day average S_{Hmax} orientations for basins in the Gulf of Thailand are also broadly consistent with the onshore stress field, ranging from N-S in the Pattani Basin to NW-SE to NNW-SSE in the Chumphon and North Malay Basins (Table 3; Figs. 4 and 5; Meyer, 2003). Hence, the present-day stress orientations obtained for basins in Thailand indicate that the fan-shaped stress field emanating from the eastern Himalayan syntaxis may, at least in the region studied herein, extend down into the Gulf of Thailand.

That forces from the eastern Himalayan syntaxis extend down to central and southern Thailand is also supported by geomorphology and trenching data, which suggest segments of major strike slip faults in western central and peninsular Thailand, particularly the Mae Ping, Three Pagodas, Ranong, Klong Marui faults, have been active through the Quaternary, with dextral motion on the NW-SE striking faults and sinistral motion on the NE-SW striking faults (Fenton et al., 2003). Furthermore, a M_b 5.6 earthquake occurred on the Ranong fault in 1978 and three GPS stations in southern Thailand, between the Ranong and Khlong Mauri faults, record 2-4 mm per year NNE motions relative to stable Sundaland, indicating current movement along these faults (Fig. 3; Shrestha, 1987; Simons et al., 2007).

The results of the stress analysis herein, coupled with the palaeostress data, is in stark contrast with interpretations from seismicity and GPS data that suggest forces exerted by the eastern Himalayan syntaxis may only extend as far as northern Thailand. The number and magnitude of recorded earthquakes in Thailand decreases southwards and large, natural earthquakes are very rare south of 17ºN latitude. Indeed, the onshore earthquakes shown to the south of 17ºN latitude in Figure 1 are thought to be the result of water loading in dams (Bott et al. 1997). The seismogenic front in Thailand approximates the southern limit of the intermontane rift basins in Northern Thailand, whereas rift basins south of this limit lie beneath a broad, flat plain that is the early stage of post-rift (thermal) subsidence. Hence, the reduction in seismicity from north to south could, on the basis of seismicity distribution alone, be interpreted to represent the outer limit of eastern Himalayan syntaxis forces being transmitted through the crust. This hypothesis is further supported by the results of GPS analysis in Indochina that reveals a significant difference in modern displacement between Thailand and the Yunnan region of China (Simons et al., 2007; Morley, 2007). Yunnan is experiencing SSW to WSW motions relative to Sundaland (including Thailand) that are associated with clockwise rotation of blocks immediately south of the eastern

Himalayan syntaxis (Simons et al., 2007). Block motion diminishes from about 12-13 mm/yr SSW in the east of Yunnan, to ~6 mm/yr WSW in the west of Yunnan, while displacements in northern Thailand are ~2-3 mm/yr to the ENE (Simons et al., 2007). Hence, the GPS data also suggest that forces associated with the eastern Himalayan syntaxis may currently have insufficient magnitude to cause measurable strain south of northern Thailand (England and Molnar, 2005). Indeed, this GPS data and distribution of seismicity has even been used to suggest that a plate boundary between Sunda and Eurasia occurs along the seismogenic front (Bird, 2003). However, despite the distribution of seismicity and GPS analysis, the present-day regional N-S S_{Hmax} orientations determined herein suggest that stresses related to the eastern Himalayan syntaxis are currently transmitted approximately 1000 km beyond the limit of seismicity in northern Thailand.

It is also interesting to note that the average stress orientations are well constrained in the Phitsanulok, Khorat, Suphan Buri and Chumphon Basins, all of which exhibit standard deviations in breakout/DIF orientations of 23-26º (Fig. 4). The S_{Hmax} orientations indicated by breakouts in the Pattani Basin also indicate an N-S average orientation, but with a higher standard deviation (40º; Fig. 4). However, the orientation of the 38 breakouts observed within the North Malay Basin are highly variable; occurring in almost all azimuths, and thus the present-day regional stress orientation in the North Malay Basin is only poorly constrained (Fig. 4). Furthermore, there is significant variation in the average stress orientations from individual wells, particularly in the Pattani and North Malay Basins, suggesting that horizontal stress magnitudes may be more isotropic in these southernmost Thai basins (Fig. 5). Hence, it is possible that the Pattani and North Malay Basin region marks a key transition zone from N-S S_{Hmax} orientations in onshore Thailand and the northern Gulf of Thailand (primarily controlled by forces generated at

372 the eastern Himalayan syntaxis) into the predominantly NW-SE to NNW-SSE S_{Hmax} orientations
373 observed in the Malay Basin (Fig. 3; Tjia & Ismail, 1994; Tingay et al., *in press*).
374
375 *Present-day Stress and the Origin of Deformation in the Gulf of Thailand*
376 The present-day geomorphology, structural style of sedimentary basins, earthquake activity and
377 stress regime all suggest that forces related to the eastern Himalayan syntaxis, and associated
378 S_{Hmax} magnitude in Thailand, diminishes southwards. The present-day stress regime in the
379 Yunnan region of China is one of significant strike-slip activity, but S_{Hmax} magnitude diminishes
380 southwards with northern Thailand being less tectonically and seismically active with the
381 predominant deformation mode being episodic mixed normal and strike-slip faulting, while
382 central and southern Thailand are tectonically quiescent. Analysis of petrophysical log, drilling
383 tests and conditions of wellbore failure in the Pattani Basin indicates a present-day normal/strike-
384 slip ($S_{Hmax} \approx S_v > S_{hmin}$) to strike-slip ($S_{Hmax} > S_v > S_{hmin}$) faulting stress regime (Meyer, 2003).
385 However, the estimated S_{Hmax} gradients of 20-22.5 MPa/km in the Pattani Basin are well below
386 the frictional limit to sliding and thus are unlikely to generate seismicity (Meyer, 2003).
387
388 The present-day stress, structural style, seismicity and geomorphological data discussed above is
389 superficially consistent with the low level of present-day tectonic activity in the Gulf of Thailand
390 and which would be expected of a post-rift basin. There is, however, an anomalous feature: the
391 presence of hundreds, if not thousands, of low displacement (~20m-300m) young normal faults
392 clearly visible on 2D and 3D seismic reflection data in the post-rift section of the Pattani and
393 North Malay Basins (Rigo de Rhigi et al., 2002; Morley et al., 2004; Fig. 6). These faults tend to
394 form extensive, 3-8 km wide curvilinear graben trends composed of conjugate convergent faults,
395 large enough to have trapped recoverable reserves of gas in the order of 27 trillion cubic feet (e.g.
396 Kornsawan and Morley 2002; Rigo de Rhigi et al. 2002, Morley et al. 2004). The post-rift fault

style is completely different from the underlying syn-rift section, which shows the typical rift style of half grabens with dominant boundary faults that display several kilometers of displacement.

Such well-developed normal faults are very unusual in a post-rift basin. The faults appear to have developed episodically during the Neogene, and some faults cut up to the sea floor. Hence this particular mode of (probably aseismic) deformation is very recent and possibly continuing today (Morley et al., 2004). The development of these faults is problematic since earthquake and borehole data indicate stress magnitudes are insufficient for failure and 10 years of GPS data indicate no differential motion across the Gulf of Thailand. However, one possible answer to this problem may lie in the episodic plate boundary effects at the Sumatra-Andaman subduction zone. The M_w 9.1, 26th December 2004, Sumatran-Andaman earthquake produced considerable differential movement of the crust on the western and eastern side of the Gulf of Thailand (Vigny et al., 2005). GPS data showed that Phuket (western side of the gulf) underwent 272 mm WSW co-seismic displacement relative to the Indian Plate, followed by 27mm of post-seismic motion in the following five days, while the eastern Khorat area (onshore eastern Thailand) underwent 37 mm WSW co-seismic motion (Vigny et al., 2005). If the recurrence interval of such an earthquake is approximately 500 years, and assuming 26 cm of differential strain across the Gulf for each event, this equates to ~10.5 km extension over a 20 my period. Such a value is sufficient to explain the amount of Miocene-Recent post-rift extension in the Gulf of Thailand.

Two moderate earthquakes (M_w= 4.7 on 27/09/2006 and M_w= 5.0 on 7/10/2006) occurred in close temporal and spatial proximity in the NW Gulf of Thailand in 2006. In records going back to 1976, the Global CMT catalog (www.globalcmt.org) does not record any other earthquakes in the Gulf of Thailand. We suggest that these earthquakes may be a delayed response to the 2004

Sumatran-Andaman earthquake. The earthquakes have a pure dip-slip normal faulting moment tensor solution and suggest a N-S S_{Hmax} orientation similar to nearby borehole breakout data.

The Sumatran-Andaman mega-thrust earthquake illustrates the potential for factors other than the eastern Himalayan syntaxis to affect deformation in Thailand. There are several large faults in the Andaman Sea (offshore continuations of the Ranong Fault and Mergui Faults) that were most active during Oligocene-early Miocene rifting, but extend to near the sea floor, indicating continued recent reactivation. The modern stress orientations are not optimally oriented for sinistral reactivation of the Ranong Fault, but the episodic perturbation of the regional stress field by mega-earthquakes, that is super-imposed upon the N-S regional stress pattern radiating from the eastern Himalayan syntaxis, may explain the observed fault activity.

Post-rift Fault Patterns in Thailand and Localized Stress Rotations

The post-rift fault zones of the Pattani and North Malay Basins provide superb examples of fault linkage geometries (Figs. 5 and 6; Rigo de Rhigi et al., 2002; Morley et al., 2004). This post-rift fault pattern is particularly striking in the North Malay Basin (Fig. 6e), where short N-S striking fault segments curve to join long NW-SE trending faults, as schematically illustrated in Figure 7. These long NW-SE striking faults are characterized by extremely high length (L) to displacement (D) ratios (up to 300:1, compared to typical 10-20:1 ratios ($D = 10^{-1}L$ to $D = 20^{-1}L$) worldwide) and tend to align along underlying syn-rift faults to form a long fault with multiple displacement highs and lows along strike, suggesting that these faults have formed by the linkage of previously isolated faults (Dawers et al., 1993; Walsh and Watterson, 1988; Morley et al., 2004). Indeed, some of these long low-displacement faults are 40-80 km long and may be composed of 20-30 linked faults that were initially 1-4 km long and typically each have maximum throws of only 100-300 m (Leo, 1997, Morley et al., 2004). Morley et al. (2004) inferred that the short N-S

faults in the North Malay Basin formed sub-parallel to the post-rift S_{Hmax} direction, while the long NW-SE faults formed by reactivation and linkage along the existing syn-rift faults. Morley et al. (2004) suggested that the reactivation of the non-optimally oriented NW-SE syn-rift faults in a N-S S_{Hmax} extensional stress regime indicated that the syn-rift faults have low cohesion or coefficient of friction.

The predominantly N-S present-day S_{Hmax} orientations determined in this study support the inferred N-S post-rift S_{Hmax} direction predicted by Morley et al. (2004) from fault patterns in the North Malay and Pattani Basins. However, breakouts in one well, drilled close to a large NW-SE trending syn-rift fault in the North Malay Basin, indicate a N-S S_{Hmax} direction at shallow depth that rotates to a WNW-ESE direction deeper, near the large NW-SE fault (Fig. 7). The observation that S_{Hmax} in this well rotates parallel to the strike of nearby syn-rift faults suggests that the post-rift reactivation of syn-rift faults may not be because they are zones of low cohesion or coefficient of friction, but instead because localized stress rotations in the vicinity of these faults renders them favorably oriented to be reactivated.

Present-day localized stress perturbations are also observed in the Pattani Basin. The average S_{Hmax} orientations for individual wells in the Pattani Basin are predominantly N-S (generally between NNE-SSW and NNW-SSE; Fig. 5b). However, S_{Hmax} orientations along the Platong-Pladang trend range from NNW-SSE to NE-SW and appear to be locally deflected to remain sub-parallel to the strike of post-rift extensional faults (Fig. 5b). Furthermore, approximately east-west S_{Hmax} orientations are observed in four wells near the Erawan Field at the southern end of the Pattani Basin, though breakouts in these four wells are elongated parallel to structure and thus may be an artifact resulting from the relatively common misinterpretation of enlarged drilling-

induced or natural fractures as breakouts on caliper log data (Fig. 5; Dart & Zoback, 1989; Meyer, 2003).

Localized stress rotations are also observed in the Phitsanulok Basin, onshore Thailand. A total of 54 breakouts and 12 DIFs were observed in 12 wells in the Phitsanulok Basin and indicate a reasonably well constrained N-S average S_{Hmax} orientation (005ºN ± 25º; Table 3). However, the stress orientations determined for individual wells reveals that the stress field appears to be locally variable within the Phitsanulok Basin (Fig. 8). Borehole breakouts indicate an approximately N-S (± 20º) S_{Hmax} orientation in eight wells examined in the Phitsanulok Basin. However, borehole breakouts in three wells suggest local stress orientations ranging from NNE-SSW to almost E-W (Fig. 8). Furthermore, 12 DIFs were observed in fractured Mesozoic quartzites in the basement within Well X that range in orientation from NNE-SSW to NE-SW, indicating a NNE SSW average S_{Hmax} orientation (034ºN ± 9º; Fig. 8).

The occurrence of small-scale stress perturbations, such as those observed in the Malay, Pattani and Phitsanulok Basins, is often considered to indicate that horizontal stress magnitudes are relatively isotropic and/or detached from primary sources of stress (Sonder, 1990; Bell, 1996; Tingay et al., 2005; Heidbach et al., 2007). However, the inference of isotropic horizontal stress magnitudes due to the presence of small-scale stress perturbations is inconsistent with the large number of breakouts and DIFs observed in this study, the recent structural styles in the region and with stress magnitudes estimated from wellbore failure (Meyer, 2003; Morley et al., *in press*). Meyer (2003) used leak-off test data and modeling of borehole breakout occurrence to estimate that a normal/strike-slip ($S_{Hmax} \approx S_v > S_{hmin}$) to strike-slip ($S_{Hmax} > S_v > S_{hmin}$) faulting stress regime is most likely present in the Pattani Basin. Furthermore, the majority of stress regimes inferred from earthquake focal mechanism solutions in onshore Thailand also suggest the

dominance of a present-day strike-slip faulting stress regime (Fig. 1). Therefore, it is unlikely that the localized stress field variations observed in the Phitsanulok, Pattani and North Malay Basins are due to isotropic horizontal stress magnitudes, nor are there any geological units in the region that are likely to act as mechanical detachment layers. However, the fault-parallel stress orientations observed in the Platong-Pladang trend and in parts of the Phitsanulok and North Malay Basins, suggest that the regional N-S S_{Hmax} stress orientation is being locally deflected by existing structures. Structures that are associated with mechanical contrasts, such as salt and shale diapirs, igneous intrusions and faults can locally perturb the stress field, with the S_{Hmax} orientation typically thought to be deflected perpendicular to mechanically stiff structures and parallel to weak structures (Yale, 1994; Bell, 1996; Tingay et al., 2006). Hence, the localized rotation in the stress field observed in the Pattani, North Malay and Phitsanulok Basins are interpreted to primarily result from the presence of mechanically weak faults.

The variable stress orientations observed in the Phitsanulok, Pattani and North Malay Basins also have important implications for hydrocarbon production. For example, Well X in northern central Thailand was drilled to estimate the potential for oil production from fractured pre-Cenozoic basement rocks under the Phitsanulok Basin. Well Z, which penetrated the fractured Mesozoic basement less than 1000 meters north of Well X, produced about 1 million barrels of oil (Fig. 9). However, subsequent wells (X, Y, W; Fig. 9) drilled to try and capitalize on this basement production were largely unsuccessful or had only minor production before watering out. Understanding the modern stress field distribution is important for determining why only one well was successful in this field. Rocks commonly contain many fractures, most of which are closed or cemented. Fractures tend to open and hydraulically conductive either as a response to the modern stress field (i.e. open fractures lie at a low angle to the maximum horizontal stress direction or are close to shear failure), or because they are propped open by being partially

mineralized (Jones and Hillis, 2003). Figure 9 shows that wells X and Y intersected predominantly NE-SW trending open fracture sets, while the successful basement producing well (Z) intersected predominantly NNW-SSE trending fractures. The local S_{Hmax} orientation in wells V and X is NE-SW to ENE-WSW; very different from the overall N-S trend in the Sirikit Field of the Phitsanulok Basin (Fig. 9). The orientation of open fractures in wells X and Y is what would be predicted from these local stress orientations. There is no borehole breakout data from well Z, but the fracture orientations from core suggest that the S_{Hmax} orientation in the vicinity of well Z has rotated to lie sub-parallel to the adjacent NNW-SSE normal fault, similar to that observed elsewhere in the Sirikit field (Figs. 8 and 9). The different local S_{Hmax} orientations and basement fracture orientations between non-producing and producing wells suggest that the NNW-SSE fractures are better connected to oil-bearing reservoir rocks, while the NE-SW to ENE-WSW trends are connected to (deeper) water-bearing strata.

Conclusions/Summary

The present-day S_{Hmax} orientations, combined with the detailed analysis of recent structural styles, provide new insight into both the large-scale and small-scale tectonic evolution of Thailand. This study undertakes the first detailed analysis of present-day stress orientation in sedimentary basins in onshore and offshore Thailand, revealing that a predominately N-S regional S_{Hmax} orientation exists throughout central and southern Thailand and the Gulf of Thailand. The regional N-S S_{Hmax} orientation is broadly consistent with stress orientations estimated from earthquake focal mechanism solutions in Northern Thailand and are interpreted to predominately reflect stresses generated by the eastern Himalayan syntaxis (Huchon et al., 1994). Hence, the N-S S_{Hmax} regional orientation and normal-strike-slip ($S_{Hmax} \approx S_v > S_{hmin}$) to strike-slip faulting stress regime ($S_{Hmax} > S_v > S_{hmin}$) observed in Thai basins is also likely to be primarily controlled by forces generated at the eastern Himalayan syntaxis. The relative absence of natural

seismicity south of northern Thailand has been previously suggested to indicate the outer limit of influence of the eastern Himalayan syntaxis on the stress pattern in SE Asia. However, the stress orientations observed from borehole breakouts and DIFs indicates that the eastern Himalayan syntaxis has a major control on the stress field up to 1000 km south of the seismically active zone.

Stress orientations observed from breakouts and DIFs in Thailand become more scattered in the southernmost Pattani and North Malay Basins, suggesting that this region may mark the transition zone in which forces other than those generated at the eastern Himalayan syntaxis become more significant. Furthermore, a well defined extensional post-rift fault pattern is observed in the Pattani and North Malay Basin that is in contrast with the strike-slip faulting stress regime predicted from stresses generated by the eastern Himalayan syntaxis. One possible other source of stress and cause of post-rift deformation in the Pattani and North Malay Basin is the Sumatran-Andaman subduction zone, with major earthquakes along this subduction zone known to have caused significant co-seismic and post-seismic displacements in central and southern Thailand (Vigny et al., 2005). Thus, we hypothesize that stresses generated along this arc may also have influenced stresses in Thailand and possibly account for the over 10 km of Miocene-Recent post-rift extension.

The post-rift sequences of Thailand offer excellent examples of present-day localized stress rotations adjacent to existing structures, with S_{Hmax} orientations often observed to be oriented sub-parallel to the strike of nearby faults. We suggest the rotation of S_{Hmax} to be sub-parallel to structure indicates that the faults are mechanically weak. Furthermore, the localized rotation of the stress field near major structures may offer an explanation for the development of long low-displacement post-rift faults striking sub-parallel to syn-rift structures in the North Malay and

Pattani Basins. The observation that these NW-SE striking faults are inconsistent with the N-S S_{Hmax} orientation predicted during post-rift times has been previously suggested to indicate that the syn-rift faults have low cohesion and coefficient of friction or that the region has undergone an additional phase of deformation in which a NW-SE S_{Hmax} orientation existed (Morley et al., 2004). However, we suggest that mechanically weak syn-rift faults may have generated small-scale stress perturbations that locally resulted in a stress orientation that is more favorable for the reactivation of syn-rift faults that propagated into the post-rift sequences.

Acknowledgments

The authors wish to thank PTT Exploration and Production and Chevron Thailand for permission to publish these results. This manuscript has benefited greatly from the detailed and constructive reviews provided by Chris Elders and Thomas Maurin. This research has been funded by the Australian Research Council.

References

Aadnøy, B.S., 1990. Inversion technique to determine the in-situ stress field from fracturing data. Journal of Petroleum Science and Engineering 4, 127-141.

Aadnøy, B.S., Bell, J.S., 1998. Classification of drill-induce fractures and their relationship to in-situ stress directions. The Log Analyst 39, 27-42.

Bell, J.S., Gough, D.I., 1979. Northeast-southwest compressive stress in Alberta: Evidence from oil wells. Earth and Planetary Science Letters 45, 475-482.

Bell, J.S., 1996. Petro Geoscience 1. In situ stresses in sedimentary rocks (part 2): applications of stress measurements. Geoscience Canada 23, 135-153.

Binh, N.T.T., Tokunaga, T., Son, H.P., Binh, M.V., 2007. Present-day stress and pore pressure fields in the Cuu Long and Nam Con Son Basins, offshore Vietnam. Marine and Petroleum Geology 24, 607-615.

Bird, P., 2003. An updated digital model of plate boundaries. Geochemistry, Geophysics, Geosystems 4, 1027, doi:10.1029/2001GC000252.

Bott, J., Wong, I., Prachuab, S., Wechbunthung, B., Hinthong, C., Surapirome, S., 1997. Contemporary seismicity in northern Thailand and its tectonic implications. In: The International Conference on Stratigraphy and Tectonic Evolution of Southeast Asia and the South Pacific, Bangkok, Thailand, pp. 453-464.

Coblentz, D., Richardson, R.M., 1995. Statistical trends in the intraplate stress field. Journal of Geophysical Research 100, 20245-20255.

Curray, J.R., 2005. Tectonics and history of the Andaman Sea region. Journal of Asian Earth Sciences 25, 187-232.

Dart, R.L., Zoback, M.L., 1989. Wellbore Breakout Analysis within the Central and Eastern Continental United States. The Log Analyst 30, 12-25.

Dawers, N.H., Anders, M.H., Scholz, C.H., 1993. Fault length and displacement: scaling laws. Geology 21, 607-614.

Ekstrom, M.P., Dahan, C.A., Chen, M.Y., Lloyd, P.M., Rossi, D.J., 1987. Formation imaging with microelectrical scanning arrays. The Log Analyst 28, 294-306.

England, P.C., Molnar, P., 2005. Late Quaternary to decadal velocity fields in Asia. Journal of Geophysical Research 110 (B12), doi:10.1029/2004JB003541.

Fenton, C.H., Charusiri, P., Hinthong, C., Lumjuan, A., Mangkonkarn, B., 1997. Late quaternary faulting in northern Thailand. In: International Conference on Stratigraphy and Tectonic Evolution of South East Asia and the South Pacific. Bangkok, Thailand, pp. 436-452.

618 Fenton, C.H., Charusiri, P., Wood, S.H., 2003. Recent paleoseismic investigations in Northern
619 Thailand. Annals of Geophysics 46, 957-981.
620 Hall, R., Morley, C.K., 2004. Sundaland Basins. In: Continent-Ocean Interactions within the East
621 Asian Marginal Seas. Clift, P. Wang, P., Kuhnt, W. and Hayes, D.E. (Eds.) AGU
622 Geophysical Monograph 149, 55-85.
623 Heidbach, O., Reinecker, J., Tingay, M., Müller, B., Sperner, B., Fuchs, K., Wenzel, F., 2007.
624 Plate boundary forces are not enough: Second- and third-order stress patterns highlighted in
625 the World Stress Map database. Tectonics 26, TC6014, doi:10.1029/2007TC002133.
626 Heidbach, O., Tingay, M., Barth, A., Reinecker, J., Kurfeß, D., Müller, B., *in press*. Global
627 crustal stress pattern based on the World Stress Map database release 2008. Tectonophysics,
628 doi:10.1016/j.tecto.2009.07.023.
629 Holt, W.E., Ni, J.F., Wallace, T.C., Haines, A.J., 1991. The active tectonics of the eastern
630 Himalayan syntaxis and surrounding regions. Journal of Geophysical Research 96 (B9),
631 14595-14632.
632 Huchon, P., Le Pichon, X., Rangin, C., 1994. Indo-China Peninsular and the collision of India
633 and Eurasia. Geology 22, 27-30.
634 Jardine, E., 1997. Dual petroleum systems governing the prolific Pattani basin, offshore
635 Thailand. Petroleum systems of S.E. Asia and Australasia Conference, Jakarta, May 21-23,
636 1997, 351-363.
637 Jones, R. M., Hillis, R.R., 2003. An integrated, quantitative approach to assessing fault-seal risk.
638 American Association of Petroleum Geologists Bulletin 87, 189-215.
639 Khan, P.K., Chakraborty, P.P., 2005. Two-phase opening of Andaman Sea: a new seismotectonic
640 insight. Earth and Planetary Science Letters 229, 259-271.
641 Kirsch, V., 1898. Die Theorie der Elastizität und die Beddürfnisse der Festigkeitslehre.
642 Zeitschrift des Vereines Deutscher Ingenieure 29, 797-807.

643 Kong, X., Bird, P., 1997. Neotectonics of Asia: thin-shell finite-element models with faults. In:
644 Yin, A. and Harrison, T.M. (Eds.), The Tectonic Evolution of Asia. Cambridge University
645 Press, New York, pp. 18-34.
646 Kornsawan, A., Morley, C.K., 2002. The origin and evolution of complex transfer zones (graben
647 shifts) in conjugate fault systems around the Funan Field, Pattani basin, Gulf of Thailand.
648 Journal of Structural Geology 24, 435-449.
649 Kozar, M.G., Crandall, G.F., Hall, S.E., 1992. Integrated structural and stratigraphic study of the
650 Khorat Basin, Rat Buri Limestone (Permian), Thailand. In: Piancharoen, C. (ed.),
651 Proceedings of National Conference on Geological Resources of Thailand, Potential for
652 Future Development, Department of Mineral Resources, Bangkok, Thailand, 682-736.
653 Lacassin, R., Hinthong, C., Siribhakdi, K., Chauviroj, S., Charoenravat, A., Maluski, H., Leloup,
654 P.H., Tapponnier, P., 1997. Cenozoic diachronic extrusion and deformation of western
655 Indochina: structure and 40Ar/39Ar evidence from NW Thailand. Journal of Geophysical
656 Research 102 (B5), 10013-10037.
657 Lacassin, R., Replumaz, A., Leloup, P.H., 1998. Hairpin river loops and slip-sense inversion on
658 Southeast Asian strike-slip faults. Geology 26, 703-706.
659 Le Dain, A.Y., Tapponnier, P., Molnar, P., 1984. Active faulting and tectonics of Burma and
660 surrounding regions. Journal of Geophysical Research, 89 B1, 453-472.
661 Leloup, P.H., Arnaud, N., Lacassin, R., Kienast, J.R., Harrison, T.M., Trong, T.T.P., Replumaz,
662 A., Tapponnier, P., 2001. New constraints on the structure, thermochronology and timing of
663 the Ailao ShaneRed River shear zone, SE Asia. Journal of Geophysical Research 106, 6683-
664 6732.
665 Leo, C.T.A., 1997. Exploration in the Gulf of Thailand in deltaic reservoirs, related to the
666 Bongkot Field. In: Fraser, A.J., Matthews, S.J., Murphy, R.W. (Eds.), Petroleum Geology of
667 Southeast Asia. Geological Society of London, Special Publication 126, 77-87.

668 Lockhart, B.E., Chinoroje, O., Enomoto, C.B., Hollomon, G.A., 1997. Early Tertiary deposition
669 in the southern Pattani Trough, Gulf of Thailand. The International Conference on
670 Stratigraphy and Tectonic Evolution of Southeast Asia and the South Pacific, Bangkok,
671 Thailand, 476-489.
672 Mastin, L., 1988. Effect of borehole deviation on breakout orientations. Journal of Geophysical
673 Research 93, 9187-9195.
674 Meyer, J.J., 2003. The determination and application of in situ stresses in petroleum exploration
675 and production. Unpublished Ph.D. Thesis, University of Adelaide, Adelaide, 237 pp.
676 Shrestha, P.M., 1987. Investigation of Active Faults in Kanchanaburi Province, Thailand.
677 Unpublished M. Sc. Thesis, Asian Institute of Technology, Bangkok, 106 pp.
678 Molnar, P., Tapponnier, P., 1975. Cenozoic tectonics of Asia: effects of a continental collision.
679 Science 189, 419–426.
680 Morley, C.K., 2001. Combined escape tectonics and subduction rollback-backarc extension: a
681 model for the Tertiary rift basins in Thailand, Malaysia and Laos. Journal of the Geological
682 Society of London 158, 461–474.
683 Morley, C.K., 2002. A tectonic model for the Tertiary evolution of strike–slip faults and rift
684 basins in SE Asia. Tectonophysics 347, 189–215.
685 Morley, C.K., 2004. Nested strike-slip duplexes, and other evidence for Late Cretaceous-
686 Paleogene transpressional tectonics before and during India-Eurasia collision, in Thailand,
687 Myanmar and Malaysia. Journal of the Geological Society of London 161, 799-812.
688 Morley, C.K., 2007. Variations in Late Tertiary–Recent strike–slip and oblique extensional
689 geometries within Indochina: the influence of pre-existing fabrics. Journal of Structural
690 Geology 29, 36–58.

691 Morley, C.K., Wonganan, N., 2000. Normal fault displacement characteristics, with particular
692 reference to synthetic transfer zones, Mae Moh Mine, Northern Thailand. Basin Research 12,
693 1-22.
694 Morley, C.K., Woganan, N., Sankumarn, N., Hoon, T.B., Alief, A., Simmons, M., 2001. Late
695 Oligocene-Recent stress evolution in rift basins of Northern and Central Thailand:
696 implications for escape tectonics. Tectonophysics 334, 115-150.
697 Morley, C.K., Haranya, C., Phoosongsee, W., Pongwapee, S., Kornasawan, A., Wonganan, N.,
698 2004. Activation of rift oblique and rift parallel pre-existing fabrics during extension and
699 their effect on deformation style: Examples from the rifts of Thailand. Journal of Structural
700 Geology 26, 1803-1829.
701 Morley, C. K., Westaway, R., 2006. Subsidence in the super-deep Pattani and Malay basins of
702 Southeast Asia: a coupled model incorporating lower-crustal flow in response to post-rift
703 sediment loading. Basin Research 18, 51-84.
704 Morley, C.K., Gabdi, S., Seusutthiya, K., 2007. Fault superimposition and linkage resulting from
705 stress changes during rifting: Examples from 3D seismic data, Phitsanulok Basin, Thailand.
706 Journal of Structural Geology 29, 646-663.
707 Morley, C.K., Charusiri, P., Watkinson, I.M., Searle, M., in press. Structural geology of Thailand
708 during the Cenozoic. In: Ridd, M., Barber A. (Eds.), The Geology of Thailand. Geological
709 Society of London Memoir.
710 Peska, P., Zoback, M.D., 1995. Compressive and tensile failure of inclined wellbores and
711 determination of in situ stress and rock strength. Journal of Geophysical Research 100,
712 12791-12811.
713 Pivnik, D.A., Nahm, J., Tucker, R.S., Smith, G.O., Nyein, K., Nyunt, M., Maung P.H., 1998.
714 Polyphase deformation in a fore-arc/back-arc basin, Salin subbasin, Myanmar (Burma).
715 American Association of Petroleum Geologists Bulletin 82 , 1837-1856.

716 Plumb, R.A., Hickman, S.H., 1985. Stress-induced borehole elongation: A comparison between
717 the Four-Arm Dipmeter and the Borehole Televiewer in the Auburn Geothermal Well.
718 Journal of Geophysical Research 90, 5513-5521.
719 Polachan, S., Pradidtan, S., Tongtaow, C., Janmaha, S., Intarawijitr, K., Sangsuwan, C., 1991.
720 Development of Cenozoic basins in Thailand. Marine and Petroleum Geology 8, 84-97.
721 Replumaz, A., Tapponnier, P., 2003. Reconstruction of the deformed collision zone between
722 India and Asia by backward motion of lithospheric blocks. Journal of Geophysical Research
723 108, doi:10.1029/2001JB00066.
724 Rigo De Rhigi, L., Baranowski, J., Chaikiturajai, C., Nelson, G., Wechsler, D., Mattingly, G.,
725 2002. Block B8/32, Gulf of Thailand Petroleum System and Implementation of Technology
726 in Field Development. Seapex Press 6, 46-55.
727 Schlumberger, 1986. Dipmeter Interpretation. New York, USA, Schlumberger Limited, 76 p.
728 Searle, M.P., Morley, C.K., in press. Tectonics and thermal evolution of Thailand in the regional
729 context of South-East Asia. In: Ridd, M., Barber A. (Eds.), The Geology of Thailand.
730 Geological Society of London Memoir.
731 Shen, Z.-K., Lu, J., Wang, M., Burgmann, R., 2005. Contemporary crustal deformation around
732 the southeast borderland of the Tibetan Plateau. Journal of Geophysical Research 110
733 (B11409), doi: 10.1029/2004JB003421.
734 Shrestha, P.M., 1987. Investigation of Active Faults in Kanchanaburi Province, Thailand.
735 Unpublished M. Sc. Thesis, Asian Institute of Technology, Bangkok, 106 pp.
736 Simons, W.J.F., Socquet, A., Vigny, C., Ambrosius, B.A.C., Abu, S.H., Promthong, C., Subarya,
737 Sarsito, D.A., Matheussen, S., Morgan, P., Spakman, W., 2007. A decade of GPS in
738 Southeast Asia: resolving Sundaland motion and boundaries. Journal of Geophysical
739 Research 112, B06420. doi:10.1029/2005JB003868.

Sonder, L.J., 1990. Effects of density contrasts on the orientation of stresses in the lithosphere: relation to principal stress direction in the Transverse Ranges, California. Tectonics 9(4), 761-771.

Tapponnier, P., Peltzer, G., Le Dain, A.Y., Armijo, R., Cobbold, P., 1982. Propagating extrusion tectonics in Asia: new insights from simple experiments with plasticine. Geology 10, 611–616.

Tapponnier, P., Peltzer, G., Armijo, R., 1986. On the mechanism of collision between India and Asia. In: Coward, M.P., Ries, A.C. (Eds.), Collision Tectonics. Geological Society of London Special Publication 19, 115-157.

Tingay, M., Müller, B., Reinecker, J., Heidbach, O., Wenzel, F., Fleckenstein, P., 2005. Understanding tectonic stress in the oil patch: The World Stress Map Project. The Leading Edge 24, 1276-1282.

Tingay, M., Müller, B., Reinecker, J., Heidbach, O., 2006. State and origin of the present-day stress field in sedimentary basins: New results from the World Stress Map Project. Golden Rocks, American Rock Mechanics Association 2006 Conference, Paper 06-1049.

Tingay, M., Reinecker, J., Müller, B., 2008. Borehole breakout and drilling-induced fracture analysis from image logs. World Stress Map Project Stress Analysis Guidelines (available online at www.world-stress-map.org).

Tingay, M., Hillis, R., Morley, C., King, R., Swarbrick, R., Damit, A., 2009. Present-day stress and neotectonics of Brunei: implications for petroleum exploration and production. AAPG Bulletin 93, 75-100.

Tingay, M., Morley, C., King, R., Hillis, R., Coblentz, D., Hall, R., *in press*. Present-day stress field of Southeast Asia. Tectonophysics, doi:10.1016/j.tecto.2009.06.019.

Tjia, H.D., Ismail, M.I, 1994. Tectonic implications of well-bore breakouts in Malaysian basins. Geological Society of Malaysia Bulletin 36, 175-186.

765 Upton, D., Bristow, C., Hurford, A.J., Carter, A., 1997. Cenozoic tectonic denudation in
766 northwestern Thailand: Provisional results from apatite fission-track analysis. In: The
767 International Conference on Stratigraphy and Tectonic Evolution of Southeast Asia and the
768 South Pacific, Bangkok, Thailand, pp. 421-431.
769 Uttamo, W., Elders, C.F., Nicols, G.J., 2003. Relationships between Cenozoic strike-slip faulting
770 and basin opening in northern Thailand. In: Storti, F., Holdsworth, R.E., Salvini, F. (Eds.),
771 Intraplate strike-slip deformation belts. Geological Society of London, Special Publication
772 210, 89-108.
773 Vigny, C., Simons, W.J.F., Abu, S., Bamphenyu, R., Satirapod, C., Choosakul, N., Subarya, C.,
774 Socquet, A., Omar, K., Abdin, H.Z., Ambrosius, A.A.C., 2005. Insight into the 2004
775 SumatraneAndaman earthquake from GPS measurements in southeast Asia. Nature 436, 201-
776 206.
777 Walsh, J.J., Watterson, J., 1988. Analysis of the relationship between displacements and
778 dimensions of faults. Journal of Structural Geology 10, 239-247.
779 Yale, D.P., 2003. Fault and stress magnitude controls on variations in the orientation of in situ
780 stress. In: Ameen M.S. (Ed.), Fracture and in-situ stress characterization of hydrocarbon
781 reservoirs. Geological Society of London Special Publication 209, pp. 55-64.
782

Tables

Table 1: Criteria for recognizing breakouts on four-arm caliper (HDT-type) logs (Plumb & Hickman, 1985).

1. Tool rotation must cease in the zone of elongation (maximum of 15° rotation within breakout).
2. There must be clear tool rotation into and out of the elongation zone (at least 30°).
3. The difference between caliper extensions must be > 6 mm.
4. The smaller of the caliper readings must be very close to bit size (±5% tolerance).
5. The length of the elongation zone must be > 1 m
6. The elongation orientation should not coincide with the high side of the borehole in wells deviated by more than 5° (±5° tolerance).

Table 2: World Stress Map (WSM) project quality ranking criteria for breakouts and drilling-induced fractures (DIFs) interpreted from four-arm caliper and image logs (Heidbach et al., *in press*). SD: standard deviation of breakout/DIF orientations.

Data Type	A-quality	B-quality	C-quality	D-quality	E-quality
Breakouts (four-arm caliper logs)	≥10 breakouts with combined length ≥300m and SD ≤12º in a single well	≥6 breakouts with combined length ≥100m and SD ≤20º in a single well	≥4 breakouts with combined length ≥30m and SD ≤25º in a single well	<4 breakouts or combined length <30m and SD ≤40º	No breakouts observed or breakouts with SD >40º
Breakouts (image logs)	≥10 breakouts with combined length ≥100m and SD ≤12º in a single well	≥6 breakouts with combined length ≥40m and SD ≤20º in a single well	≥4 breakouts with combined length ≥20m and SD ≤25º in a single well	<4 breakouts or combined length <20m and SD ≤40º	No breakouts observed or breakouts with SD >40º
DIF (image logs)	≥10 DIFs with combined length ≥100m and SD ≤12º in a single well	≥6 DIFs with combined length ≥40m and SD ≤20º in a single well	≥4 DIFs with combined length ≥20m and SD ≤25º in a single well	<4 DIFs or combined length <20m and SD ≤40º	No DIFs observed or DIFs with SD >40º

Table 3: Summary of data analyzed and stress orientation results in Thailand basins. Wells: number of wells for which image or caliper log data was examined; BO: number of breakouts observed; DIF: number of drilling-induced fractures (DIF) observed, A-E: number of A-E quality stress indicators; BO/DIF Length: total length of breakouts and DIF observed; BO/DIF Ave S_{Hmax} and SD: unweighted average maximum horizontal stress orientation (and standard deviation) from all individual breakouts and DIFs; Indicator Ave S_{Hmax} and SD: quality weighted average maximum horizontal stress orientation (and standard deviation) from stress indicators.

Basin	Wells	BO	DIF	A	B	C	D	E	Log Length (km)	BO/DIF Length (m)	BO/DIF Ave S_{Hmax}	BO/DIF SD	Indicator Ave S_{Hmax}	Indicator SD
Phitsanulok	26	54	12	3	1	1	7	14	13.5	1270	005º	25º	012º	23º
Khorat	11	130	12	3	1	4	3	1	11.6	1504	000º	26º	173º	24º
Suphan Buri	9	15	0	0	0	2	3	4	9.8	292	001º	23º	000º	16º
Chumphon	7	24	21	0	1	3	3	1	8.0	167	161º	23º	159º	17º
Pattani	42	297	0	0	8	7	23	4	70.2	8470	000º	40º	001º	25º
North Malay	11	38	0	0	1	3	1	6	11.5	382	153º	45º	159º	33º

Figure Captions

Figure 1: The main Cenozoic-Recent tectonic and structural features of the Myanmar-Western Thailand region of the back-arc mobile belt. Complied from Pivnik et al. (1998), Morley (2004) and Curray (2005).

Figure 2: Examples of borehole breakout and drilling-induced fractures (DIFs) in Thailand basins. (a) Borehole breakouts interpreted from four-arm caliper log data in the Pattani Basin. Borehole breakouts are oriented approximately 095ºN, indicating a 005ºN present-day maximum horizontal stress (S_{Hmax}) orientation. (b) DIFs observed on Formation Micro Scanner resistivity image log data in the Chumphon Basin. DIFs are oriented approximately 155ºN, indicating a 155ºN present-day S_{Hmax} orientation.

Figure 3: Present-day stress orientations, major structures and GPS-derived motions (relative to a stable Sunda plate) in onshore and offshore Thailand, Vietnam and Malaysia. There is significant scatter in stress directions between individual wells. However, the present-day stress throughout Thailand is typically oriented N-S at a basin-scale. Stress orientations from offshore Malaysia and Vietnam from Tjia & Ismail (1994) and Binh et al., (2007). Relative motions adapted from Simons et al., (2007).

Figure 4: Distribution of breakout (BOs) and drilling-induced fracture (DIFs) orientations in Thailand basins. The maximum horizontal stress is oriented perpendicular to breakouts and parallel to drilling-induced fractures. Ave S_{Hmax} Azi: average maximum horizontal stress orientation from all breakouts and DIFs; S.D: standard deviation of maximum horizontal stress orientations; L: combined total length of breakouts and DIFs.

Figure 5: Present-day maximum horizontal stress orientations in the Chumphon, North Malay and Pattani Basins, Gulf of Thailand. Stresses are locally scattered, though are typically trend between NNE-SSW and NNW-SSE and are oriented approximately N-S at the basin-scale (b) Stress orientations in the Platong-Pladang trend in the Pattani Basin. Present-day maximum horizontal stress orientations appear to be rotated sub-parallel to neighboring extensional faults and to jogs in the half graben structure.

Figure 6: Illustration of syn-rift and post-rift fault patterns in the eastern Gulf of Thailand. a) Regional syn-rift fault map of the Pattani and Khmer Basins based on 2D and 3D seismic reflection data, illustrating fault patterns in the Late Oligocene-Early Miocene syn-rift section compiled from unpublished maps made by Unocal (published in Morley et al. 2004), and Lockhart et al. (1997). b) Detail of post-rift fault swarm patterns from the Northern Pattani basin (redrawn from Rigo de Rhigi et al., 2002). c) The post-rift faults tend to form curvi-linear trends of convergent conjugate faults with 10's meters to a few hundred meters displacement. These trends often appear to be guided by underlying syn-rift faults which localize long, low-displacement post rift faults, as illustrated for the Tantawan graben. d) Time structure map for the Tantawan graben (redrawn from Rigo de Rhigi et al. 2002), absolute scale not shown (darker colors = deeper time-depths). Many of the post-rift faults tend to have different strikes from the underlying syn-rift faults but join or splay off trends controlled by the syn-rift faults. e) Example of fault map view geometry in the post-rift section from the North Malay basin (Morley et al. 2004). In d) and e) the black faults dip E to NE, while the light colored faults dip to the W to SW.

Figure 7: Schematic block diagram illustrating the interaction between post-rift and syn-rift faults, and how S_{Hmax} orientation can be related to fault orientation. The rotation in S_{Hmax}

direction with depth to be sub-parallel to syn-rift faults is illustrated from a well in the North Malay Basin.

Figure 8: Present-day stress orientations in the Sirikit Field in the Phitsanulok Basin. Present-day maximum horizontal stress orientations are predominately oriented N-S. However, stress orientations often appear to be locally rotated sub-parallel to neighboring extensional faults and drilling-induced fractures observed in Well X indicate a NE-SW stress orientation in the basement.

Figure 9: Time-structure map for the base syn-rift horizon in part of the Sirikit Field (see Fig. 9 for location). The map also shows well trajectories, pre-rift fracture orientations intersected in wells X, Y and Z, and S_{Hmax} orientation for the field. Well Z produced 1 million barrels of oil from NNW-SSE striking, open fractures in the Mesozoic quartzite basement. However, ENE-WSW oriented open fractures in wells X and Y did not produce significant volumes of hydrocarbons. We suggest that NNW-SSE striking basement fractures are more suitably oriented for tapping overlying hydrocarbon reservoirs in the regional N-S S_{Hmax} direction.

Figure 1

Click here to download high resolution image

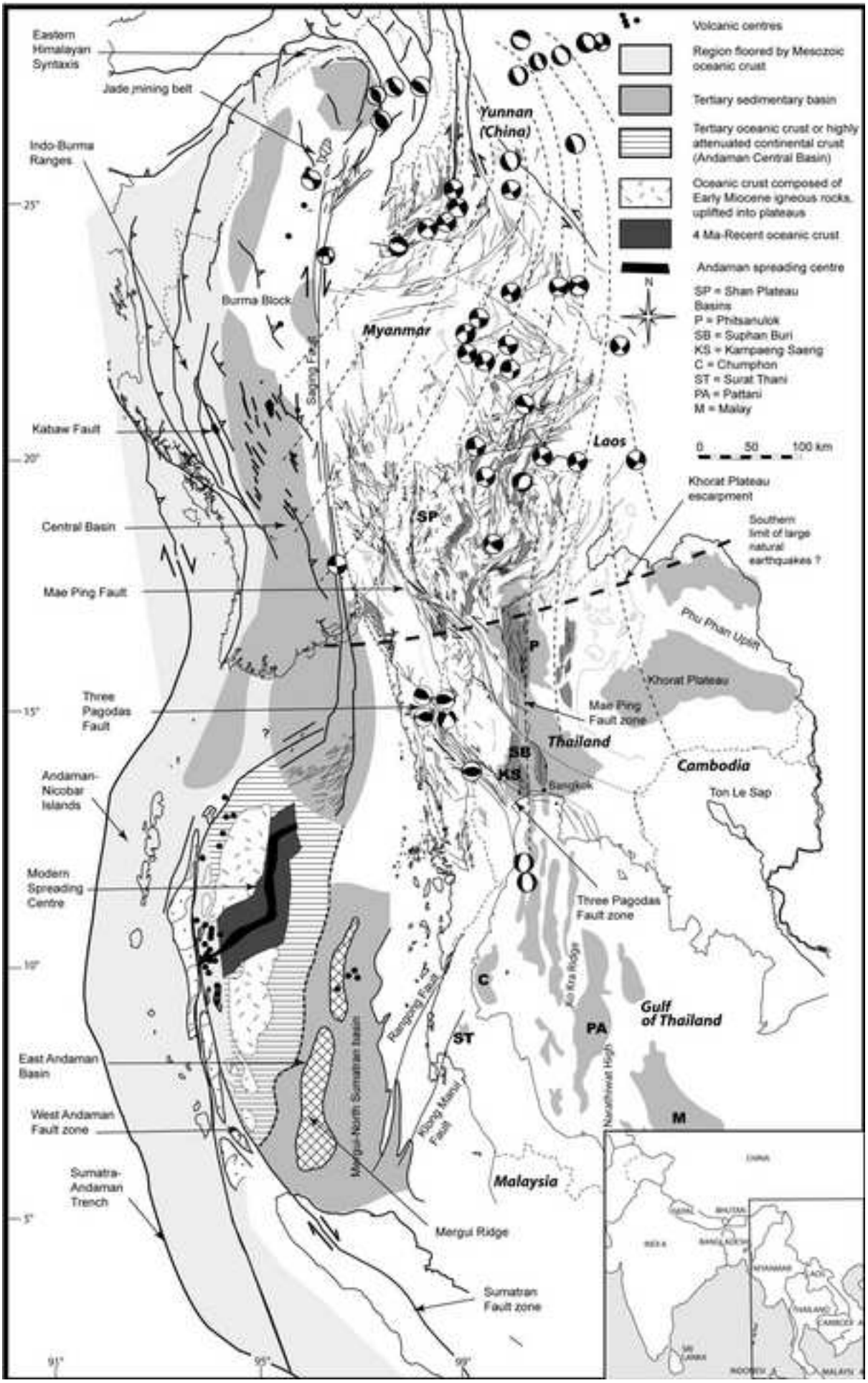

Figure 2

Click here to download high resolution image

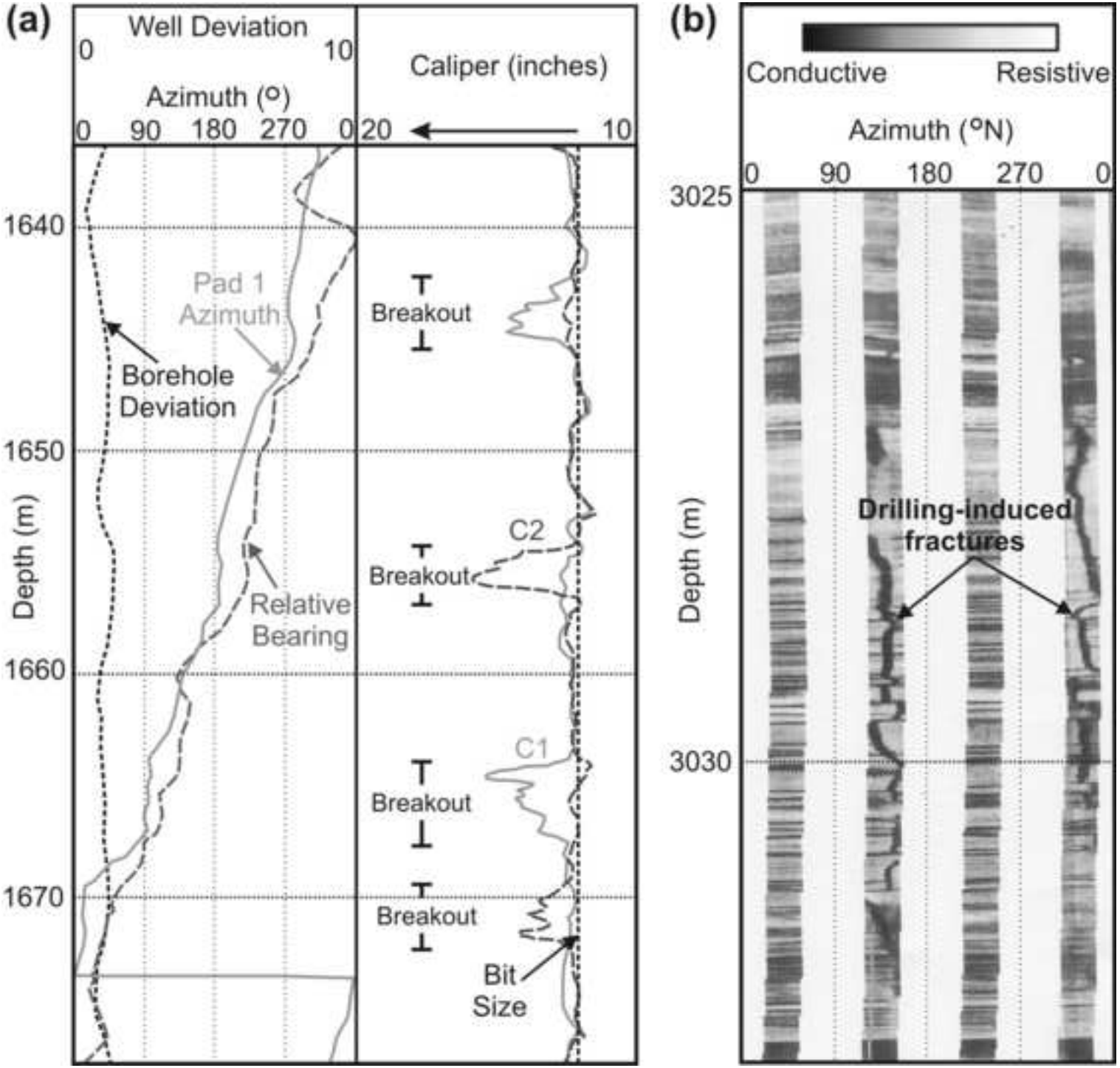

Figure 3

Click here to download high resolution image

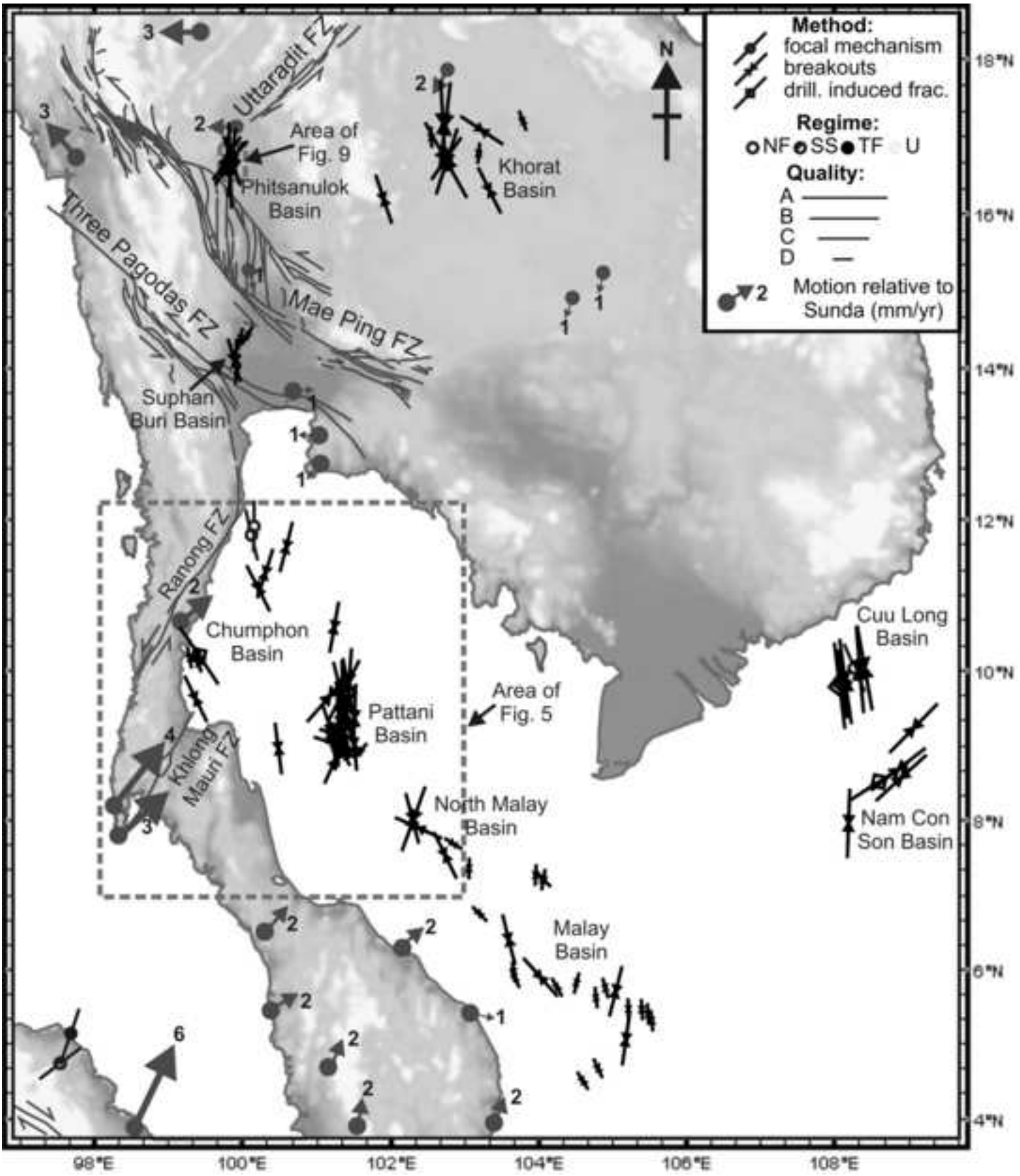

Figure 4

Click here to download high resolution image

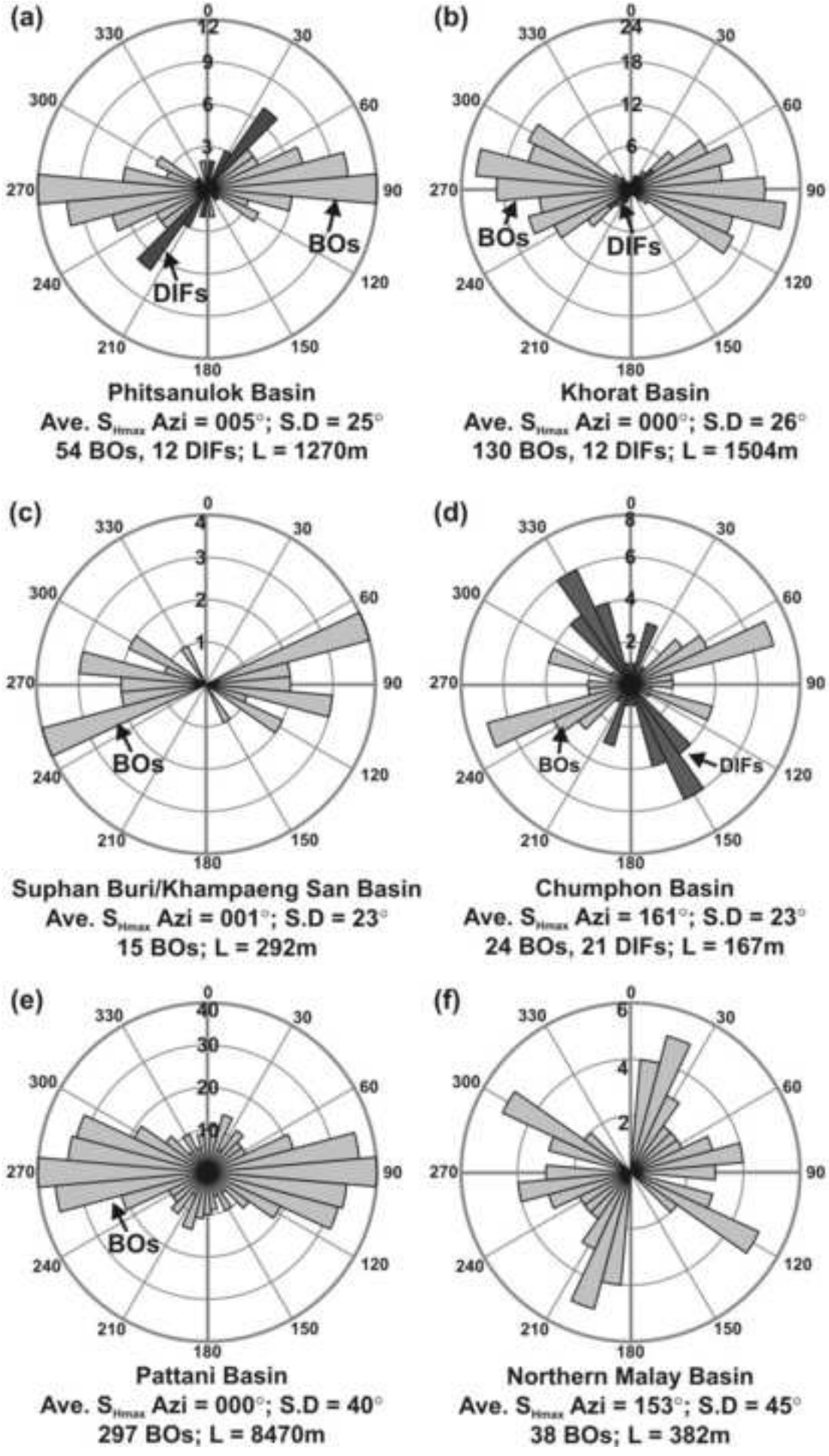

Figure 5

Click here to download high resolution image

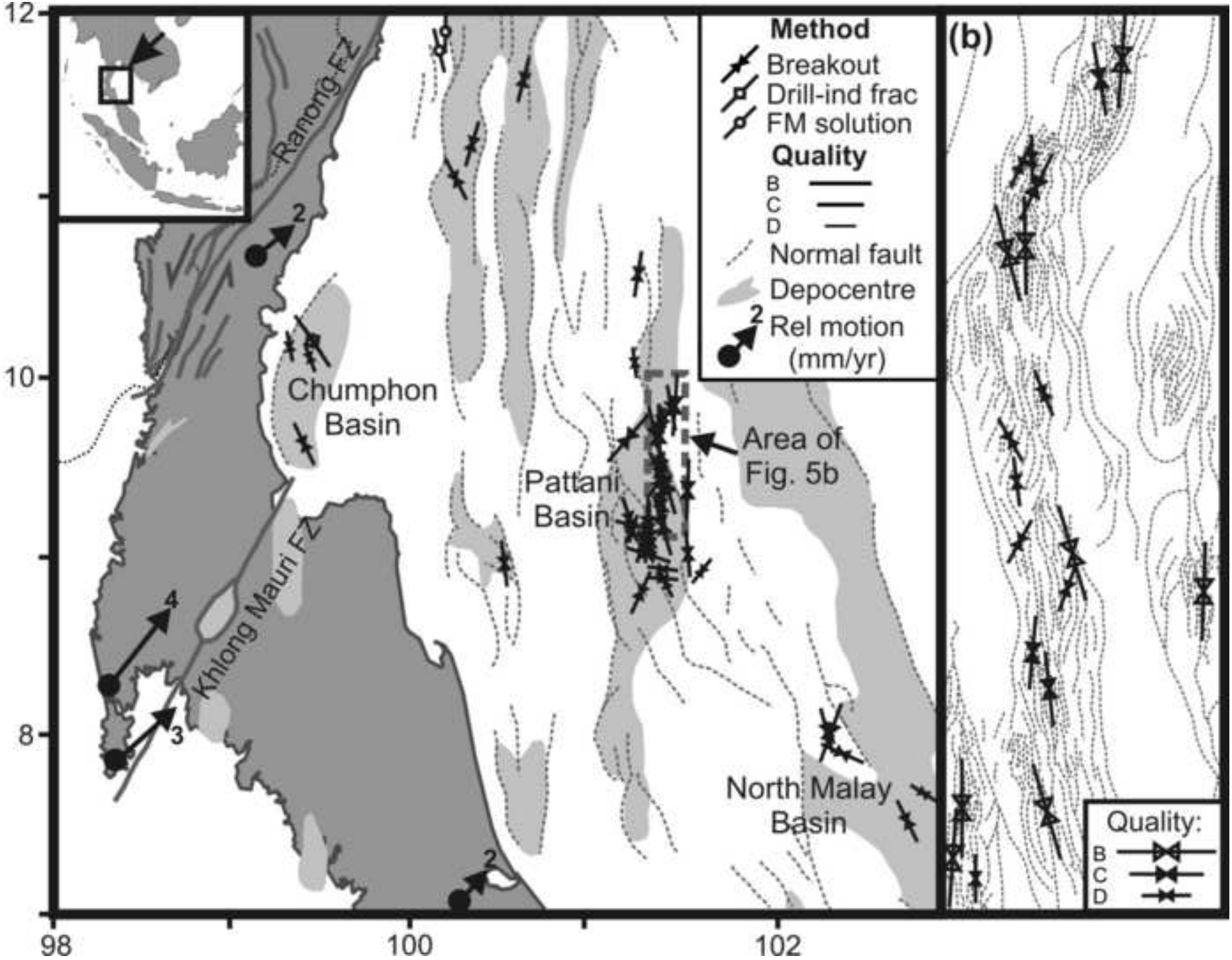

Figure 6

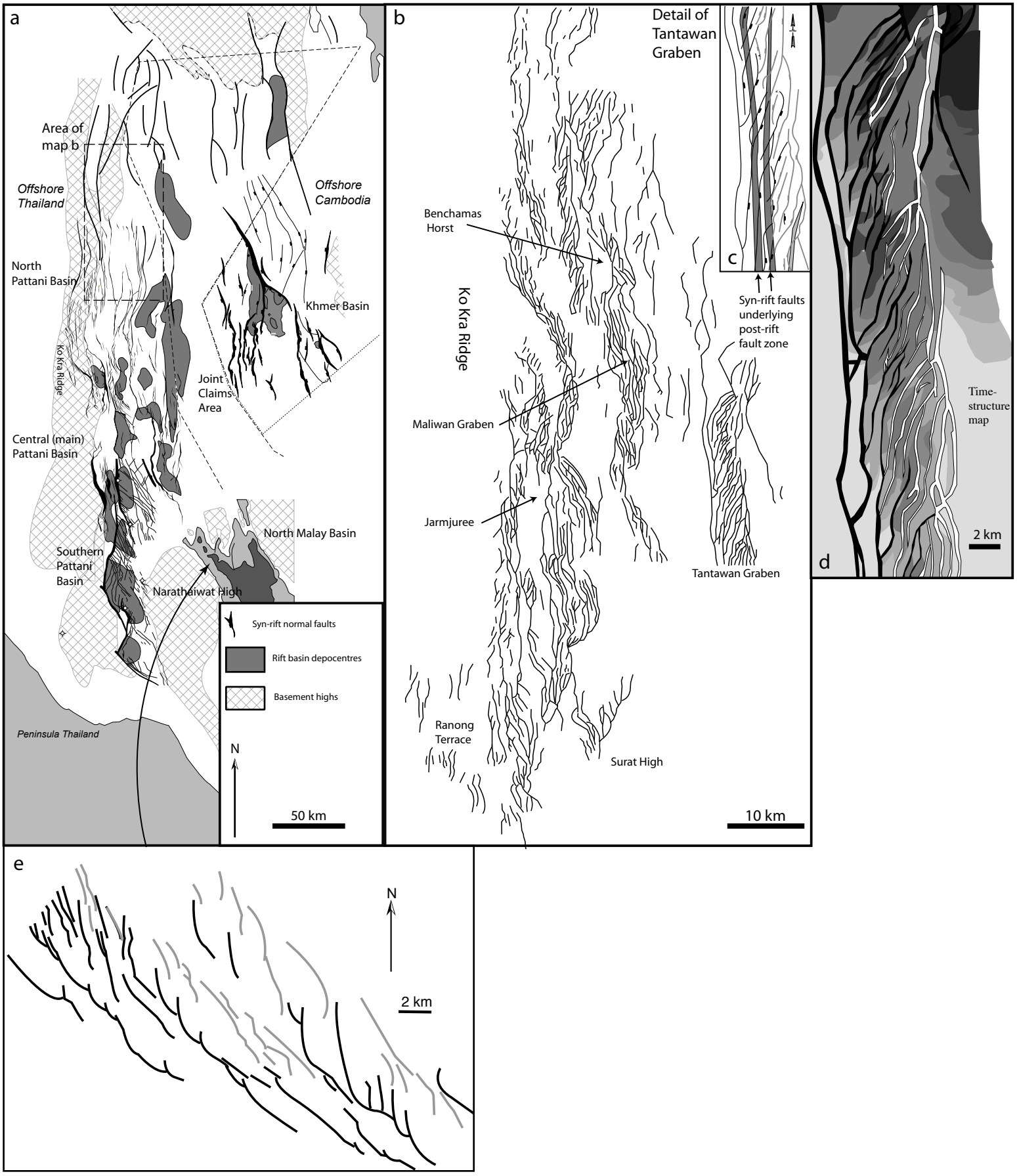
a
Area of map b
Offshore Thailand
Offshore Cambodia
North Pattani Basin
Khmer Basin
Ko Kra Ridge
Joint Claims Area
Central (main) Pattani Basin
North Malay Basin
Southern Pattani Basin
Narathaiwat High
Peninsula Thailand
Syn-rift normal faults
Rift basin depocentres
Basement highs
N
50 km
b
Detail of Tantawan Graben
Benchamas Horst
Ko Kra Ridge
Maliwan Graben
Jarmjuree
Tantawan Graben
Ranong Terrace
Surat High
10 km
c
Syn-rift faults underlying post-rift fault zone
d
Time-structure map
2 km
e
N
2 km

Figure 7

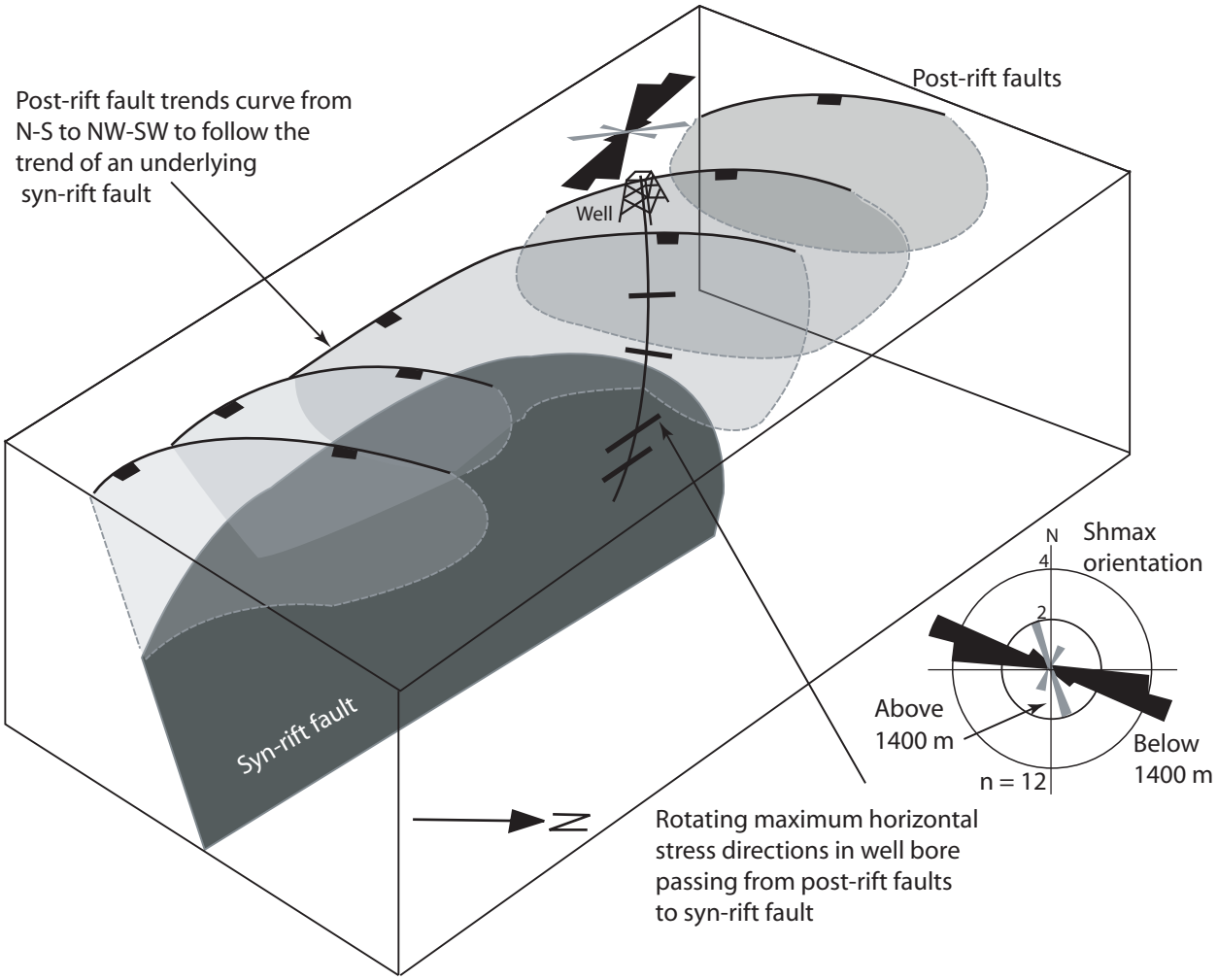
Post-rift fault trends curve from N-S to NW-SW to follow the trend of an underlying syn-rift fault
Post-rift faults
Well
Syn-rift fault
N
Shmax orientation
4
2
Above 1400 m
Below 1400 m
n = 12
Rotating maximum horizontal stress directions in well bore passing from post-rift faults to syn-rift fault

Figure 8

Click here to download high resolution image

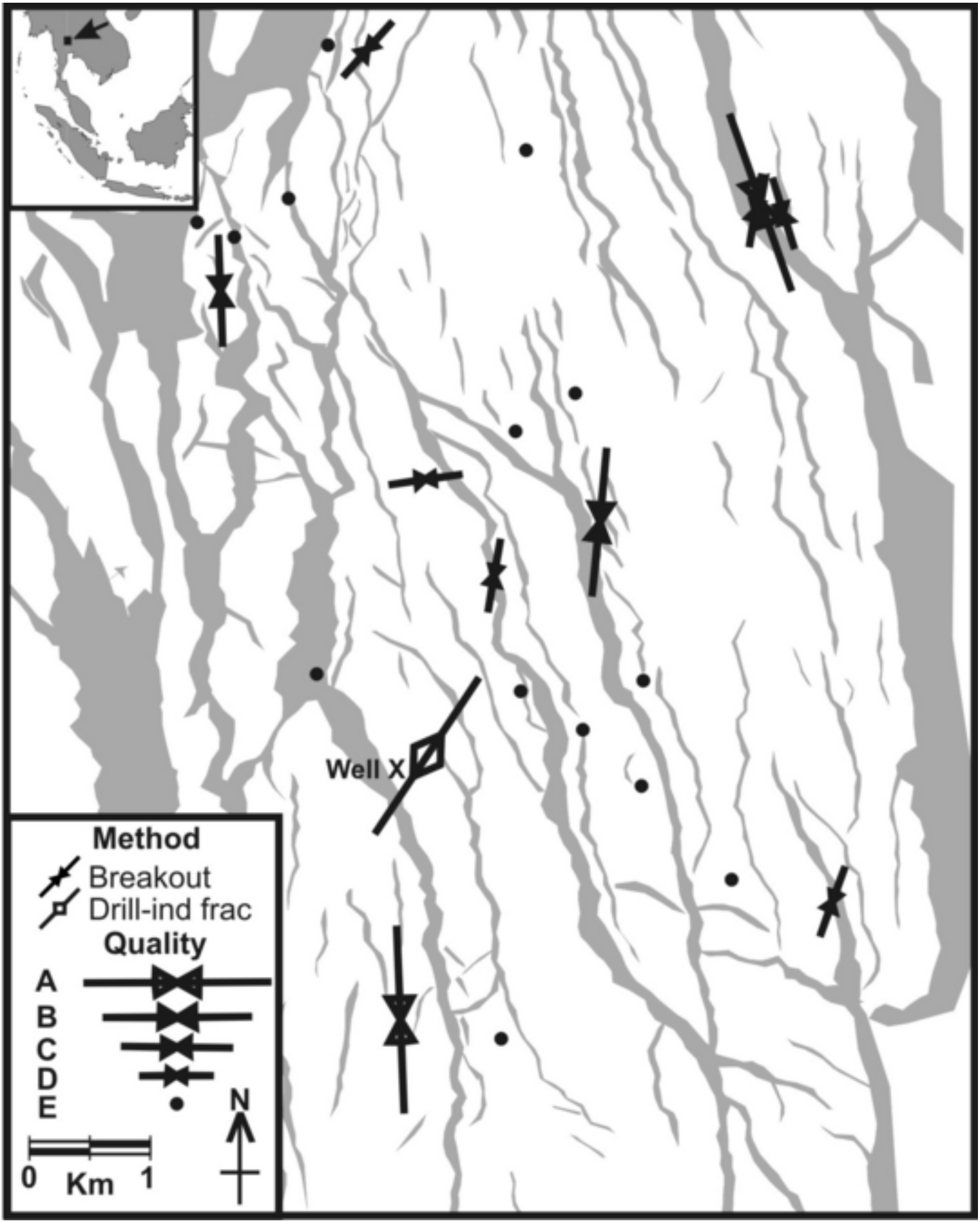

Figure 9

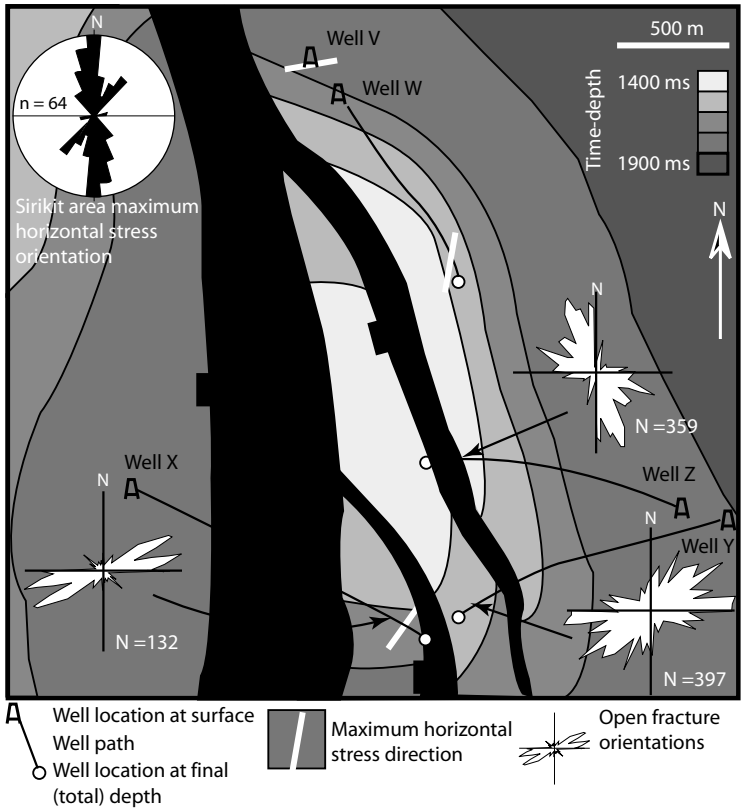
N
n = 64
Sirikit area maximum horizontal stress orientation
Well V
Well W
500 m
Time-depth
1400 ms
1900 ms
N
N
N =359
Well X
N
N =132
Well Z
N
Well Y
N =397
Well location at surface
Well path
Well location at final (total) depth
Maximum horizontal stress direction
Open fracture orientations